is $\Delta E_{i\to j} = \epsilon_j - \epsilon_i - J_{ij} + 2K_{ij}$, where ϵ, J, and K are orbital energy and Coulomb and exchange repulsion energies, respectively. Further, for transitions involving d orbitals, it is well known that the reorganization of electrons in the excited states is very large.[18] Thus, we have to compare Figure 3 with the semiempirical results of Gray et al.[16] with these points in mind.

As shown in Table VII, the Mn atom has the electron configuration $3d^{5.2}4s^{0}4p^{0.2}$. In comparison with the electronic structure of the free Mn atom $3d^{5}4s^{2}4p^{0}$, the 4s electrons delocalize over the whole complex and the 3d and 4p orbitals accept electrons from the ligands. The net charge of Mn is $+1.4 \sim +1.8$, in comparison with the formal charge +1.0. For the $Mn(CO)_5H$ complex, the 4p population is larger than those of the other complexes. The radial maximum of the 4p orbital is near the proton of the $Mn(CO)_5H$ complex, so most of the 4p population should be assigned to the hydrogen atom, as Guest et al. mentioned.[19]

Conclusion

In this paper, we studied the ^{55}Mn nuclear magnetic shielding constants of the Mn complexes $Mn(CO)_5L$ (L = H, CN, CH_3, Cl). The results of the ab initio finite perturbation method compare fairly well with the experimental chemical shifts. The paramagnetic term is a major part of the chemical shifts. In contrast to the d^{10} metals studied previously,[1] the 3d contribution gives a predominant contribution to the paramagnetic term, since the manganese atom has an incompletely occupied 3d shell. In the perturbation theoretic viewpoint, the 3d contribution arises from the transitions from the occupied $3d_\pi$ orbital to the unoccupied $3d_\sigma$ orbital. From the analysis of the interactions between these d orbitals and the ligands L, it is shown that the chemical shift due to the ligand increases (becomes more negative) with the increases in the π-donating ability and the hardness of the ligand.

The diamagnetic term is a minor part of the chemical shift, but the Pascal rule like formula, eq 1, applies as in the case of the 1B and 2B metal complexes studied previously. The ligand contribution $\sigma^{dia}(L)$ in eq 1 is the same independent of the metal to which the ligand coordinates.

After completion of this paper, the referee kindly noted that the Pasal rule like formula for the diamagnetic term shown in eq 1 is a rediscovery of an old discovery by Flygare and Goodisman in 1968.[20]

Acknowledgment. The calculations were carried out with the HITAC M200H and FACOM M382 computers at the Institute for Molecular Science and at the Data Processing Center of Kyoto University, respectively. The authors thank these computer centers for the grants of computing time.

Registry No. $Mn(CO)_5H$, 16972-33-1; $Mn(CO)_5CN$, 15602-37-6; $Mn(CO)_5CH_3$, 13601-24-6; $Mn(CO)_5Cl$, 14100-30-2; Mn, 7439-96-5.

(18) Veillard, A.; Demuynck, J. "Modern Theoretical Chemistry"; Schaefer, H. F., Ed.; Prenum Press: New York, 1977; Vol. 4, p 187.
(19) Guest, M. F.; Hall, M. B.; Hillier, I. H. *Mol. Phys.* **1973**, *25*, 629.
(20) Flygare, W. H.; Goodisman, J. *J. Chem. Phys.* **1968**, *49*, 3122.
(21) Calomon, H. J.; Hirota, E.; Kuchitsu, K.; Lafferty, W. J.; Maki, A. G.; Pote, C. S. "Structure Data of Free Polyatomic Molecules"; Landort-Boernstein: Berlin, 1976; New Series, Group II, Vol. 7.
(22) Sutton, L. E. "Table of Interatomic Distances and Configuration in Molecules and Ions"; The Chemical Society: London, 1965; Special Publication No. 18.

Electronic Structures and Reactivities of Metal–Carbon Multiple Bonds; Schrock-Type Metal Carbene and Metal Carbyne Complexes

Jiro Ushio, Hiroshi Nakatsuji,* and Teijiro Yonezawa

Contribution from the Division of Molecular Engineering, Graduate School of Engineering, and Department of Hydrocarbon Chemistry, Faculty of Engineering, Kyoto University, Kyoto 606, Japan. *Received November 25, 1983*

Abstract: The electronic structures and reactivities of the metal–carbon multiple bonds are studied for the Schrock-type carbene complex, $H_2(CH_3)Nb{=}CH_2$, and the cationic and neutral carbyne complexes, $(CO)_5Cr{\equiv}CH^+$ and $Cl(CO)_4Cr{\equiv}CH$, respectively, which show different reactivities to nucleophiles. The Fischer-type carbene complexes, $(CO)_5Cr{=}CH(OH)$ and $(CO)_4Fe{=}CH(OH)$, were studied previously. The M=C(carbene) bond in the Schrock-type complex and the Cr≡C triple bond are stronger than the M=C bond in the Fischer-type complexes. The calculated properties of these bonds agree reasonably with the available experimental data of the related compounds. The atomic charges of the carbene and carbyne carbons were calculated negative. The reactivities of the metal–carbon multiple bonds were unifiedly understood by the frontier orbital theory. For the Schrock-type complex, the HOMO has a maximum coefficient on the C_{carb} atom and the LUMO has a maximum coefficient on the Nb atom. Therefore, the electrophile attacks the C_{carb} atom and the nucleophile attacks the Nb atom. For the carbyne complexes, the differences in the reactivity between the cationic and neutral complexes were explained from the existence of the nearly degenerate LUMO and next LUMO in the frontier MO region of the neutral complex. They would never be explained by the charge-controlled mechanism.

The multiple bond between metal and carbon is of great interest as a typical bonding mode in organometallic chemistry. The formation or the breaking of these bonds is thought to be a key step in many organometallic reactions.[1-3] The compounds with a double bond between metal and carbon are called metal carbene complexes[2-5] and those with a triple bond are called metal carbyne complexes.[2,4] Further, there are two types of metal carbene complexes; one is a Fischer-type metal carbene complex in which the metal atom is in a low oxidation state,[2] the other is a Schrock-type metal carbene complex or an alkylidene complex in which the oxidation state of the metal atom is high.[3] The reactivities of these two types of complexes are different.

(1) Cotton, F. A.; Wilkinson, G. "Advanced Inorganic Chemistry", 4th ed.; Wiley: New York, 1980.
(2) Fischer, E. O. *Adv. Organomet. Chem.* **1976**, *14*, 1-32.
(3) (a) Schrock, R. R. *Acc. Chem. Res.* **1977**, *12*, 98-104. (b) Guggenberger, L. J.; Meakin, P.; Tebbe, F. N. *J. Am. Chem. Soc.* **1974**, *96*, 5420-5427. (c) Schultz, A. J.; Williams, J. M.; Schrock, R. R.; Rupprecht, G. A.; Fellmann, J. D. *J. Am. Chem. Soc.* **1979**, *101*, 1593-1595. (d) Churchill, M. R.; Youngs, W. J. *Inorg. Chem.* **1979**, *18*, 1930-1935.
(4) Fischer, E. O.; Schubert, U.; Fischer, H. *Pure Appl. Chem.* **1978**, *50*, 857-870.

0002-7863/84/1506-5892$01.50/0

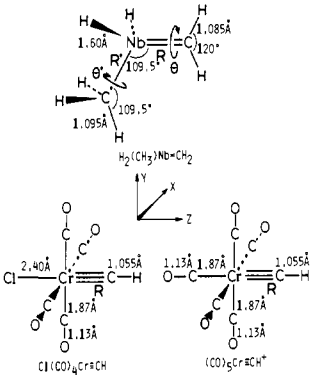

Figure 1. Geometries of $H_2(CH_3)Nb{=}CH_2$, $Cl(CO)_4Cr{\equiv}CH$, and $(CO)_5Cr{\equiv}CH^+$.

Some theoretical studies on these classes of complexes were reported previously. Spangler et al.[6] studied the geometry of $(CO)_3NiCH_2$ by sophisticated ab initio calculations. Rappe and Goddard[7] suggested that the oxo alkylidene complexes are active metathesis catalysts from the results of the GVB calculations. Nakamura and Dedieu[8] calculated $MoOCl(CH_3)(CH_2)AlH_3$ as a model for a reactive intermediate in the metathesis of olefins by the ab initio SCF-MO method. By the extended Hückel method, Goddard, Hoffman, et al.[9] discussed the origin of the abnormality of the location of the α-hydrogen in the Schrock-type complex. Block, Fenske, and Casey[10] reported approximate "non-empirical" MO calculations on the Fischer-type carbene complexes. They pointed out the importance of the LUMO of these complexes in nucleophilic attack to the carbene carbons. By the same method Kostic and Fenske[11] pointed out that the reactivity of the metal carbyne complexes is also frontier controlled.

In a previous paper in this series,[12] we studied the electronic structures and reactivities of the Fischer-type metal carbene complexes, $(CO)_5Cr{=}CH(OH)$ and $(CO)_4Fe{=}CH(OH)$, by the ab initio SCF-MO method. The nature of the metal–carbon double bond was investigated. We also studied the possible existence of the metal silylene complex, $(CO)_5Cr{=}SiH(OH)$.[13] The nature of the metal–silicon double bond was studied in comparison with the metal–carbon double bond. In the present paper, we have studied the natures and reactivities of the metal–carbon multiple bonds in the Schrock-type metal carbene complex and the carbyne complexes by the ab initio SCF-MO method. We have chosen $H_2(CH_3)Nb{=}CH_2$ as a model compound for the Schrock-type complex and have compared the properties of the M=C double bond and the reactivity with those of the Fischer-type carbene complexes. Next, we have studied the nature of the Cr≡C triple bonds in $(CO)_5Cr{\equiv}CH^+$ and $Cl(CO)_4Cr{\equiv}CH$ as model compounds for the cationic and neutral carbyne complexes, respectively. We have given a theoretical account for the different reactivities of these complexes.

In the following sections we summarize the calculational details and show the nature and the origin of the reactivity of the metal–carbon double bond of the Schrock-type carbene complex.

Table I. SCF Energies of $H_2(CH_3)Nb{=}CH_2$ and Their Singlet and Triplet Fragments[a]

molecule	total energy, au[b]
$H_2(CH_3)Nb{=}CH_2$ (R = 1.90 Å, Θ = 0°;	−3818.9535
R' = 2.07 Å, Θ' = 0°)	(−3819.1733)[c]
$H_2(CH_3)Nb$ fragment (R' = 2.07 Å, Θ' = 0°)	
singlet	−3780.1916
	−3780.1726[d]
triplet	−3780.2299
$H_2Nb{=}CH_2$ fragment (R = 1.90 Å, Θ = 0°)	
singlet (cation)	−3779.3579
doublet	−3779.6087
CH_2 fragment	
singlet	−38.5825
triplet	−38.6466
CH_3 fragment	
singlet (anion)	−39.0499
doublet	−39.2646

[a] Calculated with the MINI-1 set. [b] 1 au = 627.504 kcal/mol. [c] The value in parentheses is calculated with the MIDI-1 set. [d] The value for the excited state corresponding to the dissociation limit.

Then we go on to the metal–carbon triple bonds of the carbyne complexes.

Calculational Method

The calculational method used in this study is essentially the same as in the previous study.[12] The ab initio SCF-MO's were calculated by the Hartree–Fock–Roothaan SCF method.[14] We used a slightly modified version of the HONDO program.[15] The basis sets we used are those developed recently by Huzinaga's group.[16–18] For the Nb atom, we have used two types of basis sets, MINI-1 and MIDI-1.[16] The former is a so-called single-ζ set and the latter is single-ζ for core AO's and double-ζ for valence AO's. Each set was supplemented by the 5p AO with the same exponent as that for 5s AO. For the Cr atom, we used the MINI-2 set[17a,17b] supplemented similarly with the 4p AO. We used the MINI-1 set by Sakai et al.[17c] for Cl and the minimal 3G CGTO by Tavouktsoglou and Huzinaga[18] for C, O, and H.

The geometries of the Schrock-type carbene complex and the carbyne complexes used in the present calculations are shown in Figure 1. Though $Nb(CH_2CMe_3)_3(CHCMe_3)$ is isolated,[19,20] the structure of the complex has not been determined. Therefore, we assumed the geometry of $H_2(CH_3)Nb{=}CH_2$ as follows. The coordination about Nb was assumed to be tetrahedral. The H–Nb distance, 1.6 Å, and the geometries of the CH_2 and CH_3 ligands were estimated from those of the related compounds.[21] We investigated the changes in the electronic structure and the total energies along with the change in the $Nb{=}C_{carb}$ distance (R), the $Nb{-}C(H_3)$ distance (R'), the rotation angle around the $Nb{=}C_{carb}$ bond (θ), and the rotation angle around the $Nb{-}C(H_3)$ bond (θ').

There are two types of carbyne complexes, a cationic one and a neutral one.[4] They show different reactivities to nucleophiles. We calculated $(CO)_5Cr{\equiv}CH^+$ and $Cl(CO)_4Cr{\equiv}CH$ as model compounds of the cationic and neutral carbyne complex, respectively. The geometry of the $(CO)_5Cr$ fragment is the same as that used in the previous calculations for the Cr carbene complex, $(CO)_5Cr{=}CH(OH)$.[12] The Cl–Cr distance in $Cl(CO)_4Cr{\equiv}CH$ is the sum of the atomic radius of the Cl and Cr atoms.[22] The C–H distance in the carbyne fragment was assumed to be the same as that in acetylene. For $(CO)_5Cr{\equiv}CH^+$ we have considered the possibility of a nonlinear $Cr{\equiv}C{-}H$ bond as reported by Huttner et al.[23] We have examined two $Cr{\equiv}C{-}H$ angles, 180° and 178°.

To study the dissociation energy and the orbital correlation diagram, we have also calculated the electronic structures of the isolated fragments. They are $H_2(CH_3)Nb$, $H_2Nb{=}CH_2$, CH_2, and CH_3 for the Schrock-type

(5) Cardin, D. J.; Centikaya, B.; Lappert, M. F. *Chem. Rev.* **1972**, *72*, 545–574.
(6) Spangler, D.; Wendoloski, J. J.; Dupuis, M.; Chen, M. M. L.; Schaefer, H. F., III *J. Am. Chem. Soc.* **1981**, *103*, 3985–3990.
(7) Rappe, A. K.; Goddard, W. A., III *J. Am. Chem. Soc.* **1982**, *104*, 448–456.
(8) (a) Nakamura, S.; Dedieu, A. *Nouv. J. Chim.* **1982**, *6*, 23–30. (b) Nakamura, S.; Dedieu, A. *Theor. Chim. Acta* **1982**, *61*, 587.
(9) Goddard, R. J.; Hoffmann, R.; Jemmis, E. D. *J. Am. Chem. Soc.* **1980**, *102*, 7667–7676.
(10) Block, T. F.; Fenske, R. F.; Casey, C. P. *J. Am. Chem. Soc.* **1976**, *98*, 441–443.
(11) (a) Kostic, N. M.; Fenske, R. F. *J. Am. Chem. Soc.* **1981**, *103*, 4677–4685. (b) Kostic, N. M.; Fenske, R. F. *Organometallics* **1982**, *1*, 489–496.
(12) Nakatsuji, H.; Ushio, J.; Han, S.; Yonezawa, T. *J. Am. Chem. Soc.* **1983**, *105*, 434–440.
(13) Nakatsuji, H.; Ushio, J.; Yonezawa, T. *J. Organomet. Chem.* **1983**, *258*, C1–C4.
(14) Roothaan, C. C. J. *Rev. Mod. Phys.* **1951**, *23*, 69.
(15) King, H. F.; Dupuis, M.; Rys, J. Program Library HONDOG (No. 343) of the computer center of the Institute for Molecular Science, 1979.
(16) Sakai, Y.; Tatewaki, H.; Huzinaga, S. *J. Comput. Chem.* **1982**, *3*, 6–13.
(17) (a) Tatewaki, H.; Huzinaga, S. *J. Chem. Phys.* **1980**, *72*, 4339–4348. (b) Tatewaki, H.; Sakai, Y.; Huzinaga, S. *J. Comput. Chem.* **1981**, *2*, 96–99. (c) Sakai, Y.; Tatewaki, H.; Huzinaga, S. *J. Comput. Chem.* **1981**, *2*, 108–125.
(18) Tavouktsoglou, A. N.; Huzinaga, S. *J. Chem. Phys.* **1980**, *72*, 1385.
(19) Schrock, R. R. *J. Am. Chem. Soc.* **1974**, *96*, 6796.
(20) Schrock, R. R.; Fellman, J. D. *J. Am. Chem. Soc.* **1978**, *100*, 3359.
(21) Sutton, L. E. *Spec. Publ.-Chem. Soc.* **1958**, *No. 11*; **1965**, *No. 18*.
(22) Slater, J. *J. Chem. Phys.* **1964**, *41*, 3199.
(23) Huttner, G.; Frank, A.; Fischer, E. O. *Isr. J. Chem. 1976/1977*, *15*, 133–142.

Table II. Properties of the Nb=C_{carb} and Nb—$C(H_3)$ bonds in $H_2(CH_3)Nb{=}CH_2$

properties	Nb=C_{carb} double bond	Nb—$C(H_3)$ single bond	exptl	
			M=C_{carb}	M—$C(H_3)$
rotational barrier, kcal/mol	11.3	0.23	15.6 (Nb=C)[a]	
bond length, Å	1.89	2.07	2.026 (Ta=C)[b]	2.246 (Ta—C)[b]
bond-dissocation energy, kcal/mol	112[c]	50.3[d]	75 (Ta=C)[b]	40-60 (Ta—C)[b]
force constant				
k, mdyn/Å	5.96	5.52		
ω,[e] cm^{-1}	900-970	840-940		

[a] Value for $Cp_2Nb(CHCMe_3)Cl$ (ref 28). [b] Values for $Cp_2Ta(CH_2)(CH_3)$ (Cp = cyclopentadienyl) (ref 15). [c] Calculated from the singlet ground state of the fragments. [d] Calculated from the doublet state of the fragments. [e] The vibrational frequency was calculated from the force constant in two approximations; the atoms and groups of atoms bonded to the metal and C_{carb} or $C(H_3)$ atoms are considered to completely follow or not to follow the vibration. The former approximation gives a minimum value and the latter a maximum one.

complex and $(CO)_5Cr$, $Cl(CO)_4Cr^-$, and CH^+ for the carbyne complexes. In the dissociation reaction, the products can be singlet, doublet, or triplet for the Schrock-type complex and singlet, triplet, or quartet for the carbyne complex. The closed-shell singlet fragments were calculated by the closed-shell RHF method[14] and the multiplet fragments by the open-shell RHF method.[24] We did not consider the Jahn-Teller distortion expected in the multiplet states of the fragment.

Schrock-Type Carbene Complex

A. Properties of the Nb=C and Nb—C Bonds. Table I shows the SCF energies of $H_2(CH_3)Nb{=}CH_2$ and its closed-shell singlet, open-shell doublet, and triplet fragments. In this table we show the results obtained with the MINI-1 basis set for the Nb atom. No remarkable differences were observed as compared with the results obtained with the MIDI-1 basis set. For example, the rotational barriers of the Nb=C_{carb} bond calculated by these bases were similar as shown below. The valence MO sequences of the complex and its fragments calculated with the two basis sets were identical. Thus, in the text below we discuss only the results obtained with the MINI-1 basis set.

Table II shows some properties of the Nb=C_{carb} and Nb—$C(H_3)$ bonds, the double and single bonds. The bond lengths of the Nb—C double and single bonds are calculated to be 1.89 and 2.07 Å, respectively. In comparison with the experimental values for Ta—C double and single bonds, 2.026 and 2.246 Å, respectively, in $Cp_2(CH_3)Ta{=}CH_2$,[3a] the calculated values are shorter by 0.2 Å, but the difference between the double and single bond lengths, about 0.2 Å, is the same. This difference is close even to the difference in the C–C single and double bonds in ethane (1.536 Å) and ethylene (1.339 Å). However, different metal–carbon single and double bond lengths in the Nb and Ta complexes are also reported on the basis of the X-ray or neutron diffraction experiments. Guggenberger et al. reported 2.32 Å for the Nb—C single bond in $Cp_2Nb(C_2H_5)(C_2H_4)$,[3b] Schultz et al. reported 1.90 Å for the Ta—C double bond in $[Ta(CHCMe_3)(PMe_3)Cl_3]_2$,[3c] and Churchill and Youngs reported 1.93 or 1.96 Å for the Ta—C double bonds in $Ta(CHCMe_3)_2(mesityl)(PMe_3)_2$.[3d] We think these lengths are not appropriate for comparing with the present results, because the Nb–C single bond length in $Cp_2Nb(C_2H_5)(C_2H_4)$ is longer than the standard Ta—C(alkyl) single bond length, ~2.25 Å.[3c] For the double bond, the compounds are very much different from the present complex, because $[Ta(CHCMe_3)(PMe_3)Cl_3]_2$ is a dinuclear complex and $Ta(CHCMe_3)_2(mesityl)(PMe_3)_2$ has two M—C bonds centered on the same Ta atom.

In Table II, the force constants for the vibration of only the Nb–C bonds are given. The vibrational frequencies were calculated in two different ways which would correspond to the upper and lower limits of the vibrational frequency (see footnote *d*). The frequency of the double bond is a little larger than that of the single bond. The vibrational frequency for the Schrock-type Nb=C_{carb} bond is about twice as large as those of the Fischer-type Cr=C_{carb} and Fe=C_{carb} bonds.[12]

The bond-dissociation energy of the Nb=C_{carb} bond in the $H_2(CH_3)Nb{=}CH_2$ to the closed-shell singlet fragments, $H_2(CH_3)Nb$ and CH_2, is calculated to be 112 kcal/mol from the SCF energies in Table I. The corresponding values for the Fischer-type carbenes, $(CO)_5Cr{=}CH(OH)$ and $(CO)_4Fe{=}CH(OH)$, were 44.4 and 36.8 kcal/mol, respectively.[12] This shows that the metal carbene double bond is stronger in the Schrock-type complexes than in the Fischer-type complexes. This is reflected also in the equilibrium bond length and the force constant. The experimental bond energy of the Ta=C_{carb} bond is 75 kcal/mol[3] and that of the C=C bond in ethylene is 136 kcal/mol when it dissociates into two singlet carbenes.[25] On the other hand, the dissociation energy of the Nb–C single bond for homolytic fission (doublet dissociation) is calculated to be 50 kcal/mol, which compares reasonably with the experimental energy, 40–60 kcal/mol, of the Ta–$C(H_3)$ bond in $Cp_2(CH_3)Ta{=}CH_2$.[26]

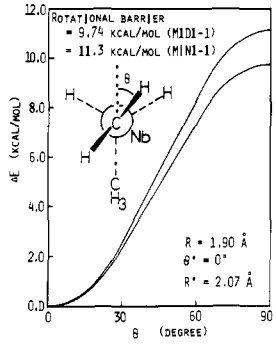

Figure 2. Potential curve for the rotation around the Nb=C_{carb} bond of $H_2(CH_3)Nb{=}CH_2$. See Figure 1 for the definition of R, θ', and R'.

The dissociation of the Nb=C_{carb} bond to the triplet fragments is also of interest. It was calculated to be 48.3 kcal/mol. As pointed out in our previous work,[12] this theoretical value should be an underestimate, since the magnitude of the correlation energy in a closed-shell singlet state should be larger than that in an open-shell triplet state. In order to estimate a correct value, the electron correlation should be taken into account. On the other hand, for singlet dissociations, which involve only closed-shell electronic states, we may expect a cancellation of correlation energy between initial and final states, and therefore, the effect of electron correlation would be small. Then, we wil analyze the Nb=C double bond by the correlation diagram involving only the singlet fragments. However, we also note that the dissociation into the triplet fragments could be a stable dissociation path of the Nb=C_{carb} bond. The reaction paths should be similar to the non-least-motion and least-motion paths[27] in the dimerization reactions of two singlet and triplet CH_2, respectively, to form ethylene.

(24) Roothaan, C. C. J. *Rev. Mod. Phys.* **1960**, *32*, 179.

(25) (a) The C=C bond-dissociation energy of ethylene to the triplet carbenes is 120 kcal/mol (ref 25b). The triplet carbene is more stable than the singlet one by 8 kcal/mol. (b) Vedeneyev, V. I.; Gurvich, L. V.; Kondrat'yev, V. N.; Medvedev, V. A.; Frankevich, Ye. L. "Bond Energies, Ionization Potentials and Electron Affinities"; translated by Price, W. C.; Edward Arnold: London, 1966.

(26) Schrock, R. R.; Parshall, G. W. *Chem. Rev.* **1976**, *76*, 243–268.

(27) Hoffmann, R.; Gleiter, R.; Mallory, F. B. *J. Am. Chem. Soc.* **1970**, *92*, 1460–1466.

Table III. Orbital Energies and Coefficients of Some Important MO's of $H_2(CH_3)Nb{=}CH_2$ and Its Singlet Fragments, $H_2(CH_3)Nb$ and CH_2[a]

	$H_2(CH_3)Nb{=}CH_2$			$H_2(CH_3)Nb$[b]		CH_2	
	Nb=C (σ)	HOMO (π)	LUMO (π)	HOMO (π)	LUMO (σ)	HOMO (σ)	LUMO (π)
ϵ_i, eV	−11.303	−7.801	2.111	−7.013	1.348	−8.550	4.691
Nb							
$4d_{x^2}$	0.12	0.0	−0.68	0.0	−0.22		
$4d_{y^2}$	−0.33	0.0	0.43	0.0	−0.35		
$4d_{z^2}$	0.42	0.0	0.12	0.0	0.20		
$4d_{xy}$	0.0	0.23	0.0	0.51	0.0		
$4d_{xz}$	0.0	0.49	0.0	0.84	0.0		
$4d_{yz}$	−0.18	0.0	−0.36	0.0	0.04		
5s	0.17	0.0	0.0	0.0	0.68		
$5p_x$	0.0	0.34	0.0	0.21	0.0		
$5p_y$	0.09	0.0	0.59	0.0	−0.18		
$5p_z$	−0.04	0.0	−0.35	0.0	0.77		
C(carbene)							
2s	0.11	0.0	0.07			0.49	0.0
$2p_x$	0.0	0.57	0.0			0.0	1.0
$2p_y$	0.04	0.0	−0.06			0.0	0.0
$2p_z$	−0.56	0.0	0.09			−0.85	0.0
C(methyl)							
2s	−0.04	0.0	0.11	0.0	−0.11		
$2p_x$	0.0	0.02	0.0	0.06	0.0		
$2p_y$	−0.22	0.0	−0.16	0.0	0.0		
$2p_z$	−0.02	0.0	−0.03	0.0	−0.10		

[a] See Figure 1 for the coordinates. [b] The singlet excited state corresponding to the dissociation limit.

Figure 1 shows the most stable conformation of $H_2(CH_3)Nb{=}CH_2$. It defines the zeros of the rotational angles θ and θ'. Figure 2 shows the potential curve for the rotation θ around the $Nb{=}C_{carb}$ bond. The $Nb{=}C_{carb}$ distance (R), the $Nb{-}C(H_3)$ distance (R'), and the rotation angle around the $Nb{-}C(H_3)$ bond (θ') were fixed at 1.90 Å, 2.07 Å, and 0°, respectively. Two curves correspond to the results obtained with MINI-1 and MIDI-1 basis sets for the Nb atom. The rotational barrier was calculated to be 9.7 kcal/mol for the MIDI-1 set and 11.3 kcal/mol for the MINI-1 set, which are comparable with the observed value, 15.6 kcal/mol, from the proton NMR experiment on the complex $Cp_2Nb(CHCMe_3)Cl$.[28] These theoretical values are larger than those obtained previously for the Fischer-type complexes, namely, 0.41 kcal/mol for the Cr carbene complex and 2.94 kcal/mol for the Fe carbene complex.[12] This trend agrees with the result that the $M{=}C_{carb}$ bond is stronger in the Schrock-type complexes than in the Fischer-type complexes. On the other hand, for the Nb–C single bond, the barrier to rotation is calculated to be 0.23 kcal/mol. It is essentially of the order of free rotation, as expected.

B. Correlation Diagram. Figure 3 shows a correlation diagram of the orbitals of $H_2(CH_3)Nb{=}CH_2$ with those of its singlet fragments, and Table III shows the orbital energies and coefficients of some important MO's of the complex and the fragments. In the $H_2(CH_3)Nb$ fragment, three of the five valence electrons of the Nb atom are used to make bonds between Nb and methyl and between Nb and two hydrogens. The other two valence electrons of the Nb atom occupy a d_π-type lone-pair MO which constitutes the HOMO of the $H_2(CH_3)Nb$ fragment. Here, d_π means a d_{xz} orbital of the Nb atom (see Figure 1). The d_δ (d_{xy}) and $5p_x$ AO's also mix with the HOMO. The LUMO of the $H_2(CH_3)Nb$ fragment is mainly the $5s\,5p_\sigma$ hybrid orbital with a small nature of the d_σ orbital, σ expressing a direction of the $Nb{=}C_{carb}$ bond. The HOMO of the CH_2 fragment is sp_σ-hybrid lone-pair orbital, and the LUMO is a pure p_π orbital, π expressing a direction perpendicular to the CH_2 plane. These frontier MO's are illustrated in the left- and right-hand sides of Figure 3. The orbitals of the $Nb{=}C_{carb}$ bond of $H_2(CH_3)Nb{=}CH_2$ are correlated with these orbitals of each fragment as follows. The σ bond of the $Nb{=}C_{carb}$ double bond is formed by an electron transfer from the HOMO of the carbene CH_2 fragment to the LUMO of the $H_2(CH_3)Nb$ fragment and the bond is essentially a d_σ-(Nb)–sp_σ(C) bond. The π bond is formed through a π back transfer of an electron from the HOMO of $H_2(CH_3)Nb$ to the LUMO of CH_2, and the bond is essentially a $d_\pi,5p_\pi$(Nb)–p_π(C) bond. The most stable conformation of $H_2(CH_3)Nb{=}CH_2$ is determined by a maximum overlap between the $d_\pi,5p_\pi$ AO's on Nb of $H_2(CH_3)Nb$ and the p_π AO on carbon of CH_2. In this conformation, the π back transfer interaction becomes maximum.

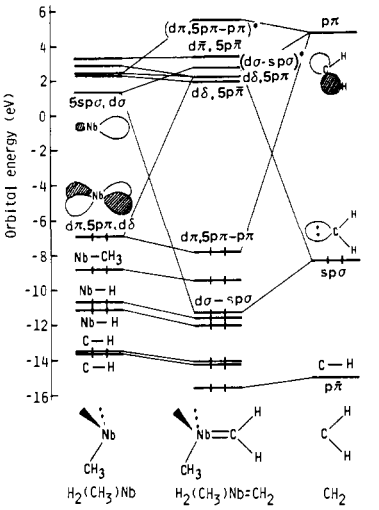

Figure 3. Correlation diagram of the orbitals of $H_2(CH_3)Nb{=}CH_2$ with those of the singlet fragments.

The origin of the rotational barrier around the $Nb{=}C_{carb}$ bond, which is much larger than those around the $Cr{=}C_{carb}$ and $Fe{=}C_{carb}$ bonds of the Fischer-type complexes, is understood from the orbital correlation diagram (Figure 3). The difference between the Schrock- and Fischer-type complexes is due to the difference in the frontier orbitals between the $H_2(CH_3)Nb$ fragment and $(CO)_5Cr$ and $(CO)_4Fe$ fragments. As reported previously, the smallness of the rotational barrier of the Fischer-type complexes is due to the degenerate (or almost degenerate) nature of the d_π- and $d\pi$-type MO's of the fragment, $(CO)_5Cr$ or $(CO)_4Fe$.[12] (Here, a $d\pi$ orbital means a d orbital obtained by a rotation of the d_π orbital by 90° around the metal–carbon bond.) Without any change in energy, these degenerate MO's can form a new set of degenerate MO's by an orthogonal transformation, keeping the overlap between the d_π AO of Cr or Fe and the p_π AO of CH_2 maximum as the CH_2 fragment rotates. On the other hand, for the $H_2(CH_3)Nb$ fragment there is no $d\pi$ orbital degenerate or

(28) Schrock, R. R.; Messerle, L. W.; Wood, C. D.; Guggenberger, L. J. *J. Am. Chem. Soc.* **1978**, *100*, 3793–3800.

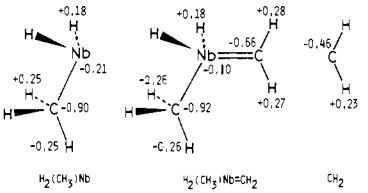

Figure 4. Net gross atomic charges in $H_2(CH_3)Nb{=}CH_2$ and its singlet fragments.

Table IV. σ and π AO Populations of the Carbene Fragment in the Free State and in $H_2(CH_3)Nb{=}CH_2$

ligand	free	$H_2(CH_3)Nb{=}CH_2$[a]
CH_2 carbene		
σ	8.0	7.188 (−0.812)
π	0.0	0.916 (+0.916)

[a] Values in parentheses show the amounts of the transfer (negative) and back transfer (positive).

almost degenerate with the d_π orbital. The $d\pi$ AO on the Nb atom is already used for the Nb–C(H_3) bond. We note that the calculated barrier of 11.3 kcal/mol arises mainly from the difference in the bonding of the d_π AO with CH_3 and with H. When the CH_3 group of the $H_2(CH_3)Nb$ fragment is replaced with H, the d_π and $d\pi$ AO's become degenerate so that the barrier to rotation should become much smaller. Thus, we further understand that the barrier to rotation should be very much dependent on the difference in the ligands on the Nb atom. In the case of $Cp_2(CH_3)Nb{=}CH_2$, the d_π orbital is used for the Cp–Nb bond more tightly than the $d\pi$ orbital used for the CH_3–Nb bond.[29] Therefore, the HOMO of the $Cp_2(CH_3)Nb$ fragment becomes $d\pi$ in nature and the stable conformation of CH_2 becomes different from the present case by 90°.[30]

C. Charge Distribution. In our previous paper, we analyzed the charge distributions of the Fischer-type complexes and showed that the M=C bond in the Fischer-type complexes polarized into $M(\delta+){=}C(\delta-)$.[12] Figure 4 shows the charge distributions of $H_2(CH_3)Nb{=}CH_2$ and its fragments. The carbene carbon atom in the complex has a negative charge of 0.66, and the Nb atom whose formal charge is 3+ is also negatively charged. Though the absolute values of the atomic charges based on the population analysis are sometimes questionable and can even be counterintuitive,[31] we are confident that the C_{carb} is negatively charged, because the methyl carbon whose environment in the complex is not much different from that around the C_{carb} has reasonable negative charge, 0.92−. The carbon atom in methane calculated with the same basis set has negative charge, 0.94−.

Table IV shows the σ and π AO populations of the carbene fragment in the free state and in the complex. The amounts of the σ- and π-electron transfers between the fragments are as large as 0.81 and 0.91, respectively. In the Fischer-type complexes, for example $(CO)_5Cr{=}CH(OH)$, the amounts of the σ and π transfers between Cr and C_{carb} were 0.191 and 0.187, respectively.[12] Goddard et al. explained this large amplitude of the π back transfer as due to the large overlap integral between the d_π AO of Nb and the p_π AO of C_{carb}.[9] The large charge transfer may be an origin of the strong $Nb{=}C_{carb}$ bond. Table V shows the valence AO populations on the metal atom. Due to the formation of the complex from its singlet fragments, the d_σ (d_{z^2}) AO population increases and the d_π (d_{xz}) AO population decreases corresponding to the σ transfer and the π back transfer.

In order to see the relation between the charge distribution and the reactivity of the carbene carbon atoms, we analyzed the charge on the carbene carbon atom into σ and π components. The data are shown for both Schrock- and Fischer-type complexes, their fragments, and also ethylene in Table VI. Though all the carbon atoms analyzed here have negative atomic charge, a large difference is seen in the π component. (The difference in the total atomic charge depends mainly on the difference in the π component.) The population in the π region of the carbene carbon atom of $H_2(CH_3)Nb{=}CH_2$ is 0.916 and is close to the population of the carbon of ethylene, 1.000. On the other hand, the π AO population of the carbene carbon atom of the Fischer-type complex, $(CO)_5Cr{=}CH(OH)$, is 0.484. Therefore, when a nucleophilic reagent approaches the Fischer-type complex, it can see the nuclear positive charge of the carbon if it is in the π direction. However, for the Schrock-type complexes, the carbene carbon is well shielded in all directions. This may explain the difference in the reactivity of these two types of carbene complexes, though a more complete explanation is given, in the next section, by the frontier orbital theory.

Table V. Valence AO Populations of the Nb Atom of $H_2(CH_3)Nb{=}CH_2$ and Its Fragment[a,b]

AO	complex	fragment[c]
$4d_{x^2}$	0.53	0.41
$4d_{y^2}$	0.53	0.45
$4d_{z^2}$	0.66	−0.01
$4d_{xy}$	0.75	1.07
$4d_{xz}$	1.11	1.84
$4d_{yz}$	0.35	0.29
sum	3.93	4.07
5s	0.50	0.61
$5p_x$	0.54	0.36
$5p_y$	0.13	0.15
$5p_z$	0.09	0.06
sum	1.26	1.18

[a] See Figure 1 for the coordinates. [b] The electron configuration of the free Nb atom is d^4s^1. [c] Values for the singlet state corresponding to the dissociation limit.

Table VI. Analysis of the Charge of the Carbene Carbon Atom

molecule[a]	population π	σ	$\pi+\sigma$	atomic charge
$H_2(CH_3)Nb{=}C^*H_2$	0.916	5.742	6.658	−0.658
C^*H_2 fragment	0.0	6.463	6.463	−0.463
$(CO)_5Cr{=}C^*H(OH)$	0.484	5.710	6.194	−0.194
$C^*H(OH)$ fragment	0.321	5.837	6.158	−0.158
$H_2C{=}C^*H_2$	1.000	5.519	6.519	−0.519

[a] The charge on the carbon with an asterisk is analyzed.

D. Reactivity. The Schrock-type complex is readily attacked by an electrophilic reagent at the carbene carbon atom, and a nucleophilic reagent attacks the metal atom, not the carbene carbon atom, e.g., electrophilic attack on the carbene carbon[3]

$$Cp_2(CH_3)Ta{=}CH_2 + AlMe_3 \rightarrow Cp_2(CH_3)Ta{-}CH_2AlMe_3$$

nucleophilic attack on the metal atom[20]

$$(Me_3CCH_2)_3Nb{=}CHCMe_3 + CH_3C(O)Cl \rightarrow (Me_3CCH_2)_3Nb(Cl)OC(CH_3){=}CHCMe_3.$$

On the other hand, the Fischer-type complex is readily attacked by a nucleophilic reagent at the carbene carbon atom. We have shown in a previous paper[12] that this reactivity of the Fischer-type complex is not explained by the charge control but by the frontier orbital control.

For the Schrock-type complexes, it seems that the experimental reactivity of the carbene carbon atom may be explained by the idea of the charge control, since C_{carb} is negatively charged and the metal atom is less negatively charged. However, C_{carb} is not the most negative among the atoms constructing this complex. The C(H_3) atom is more negative than the C_{carb} atom. In addition, the charge of the metal atom which a nucleophile easily attacks is not positive, but calculated to be negative. The idea of the charge control of the reaction does not explain why an electrophile attacks C_{carb}, not C(H_3), and why a nucleophile attacks the Nb atom.

(29) Lauher, J. W.; Hoffmann, R. *J. Am. Chem. Soc.* **1976**, *98*, 1729–1742.
(30) (a) Guggenberger, L. J. *Inorg. Chem.* **1973**, *12*, 294–301. (b) Guggenberger, L. J.; Schrock, R. R. *J. Am. Chem. Soc.* **1975**, *97*, 6578–6579.
(31) Ammeter, J. H.; Burgi, H.-B.; Thibeault, J. C.; Hoffmann, R. *J. Am. Chem. Soc.* **1978**, *100*, 3686.

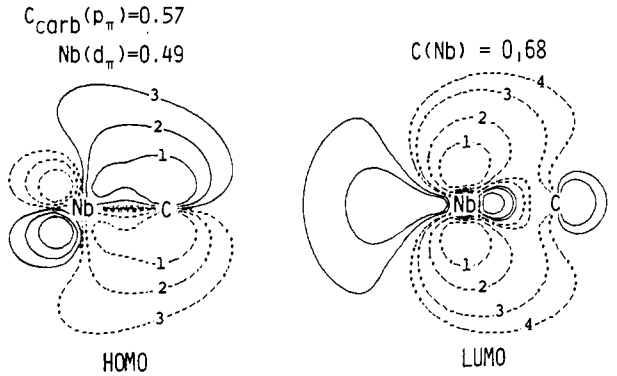

Figure 5. Contour maps of the frontier orbitals of $H_2(CH_3)Nb{=}CH_2$. The intersection is perpendicular to the plane of the carbene group and includes the $Cr{=}C_{carb}$ bond. Solid and broken lines correspond to plus and minus signs in the MO's. The numbers 1–4 on the contours correspond to the values (au) 0.1, 0.05, 0.02, 0.01, respectively. Above each map, the dominant coefficients of the orbital are shown.

According to the frontier orbital theory by Fukui et al,[32] the primary feature of electrophilic and nucleophilic reactions is governed by the HOMO and the LUMO, respectively, of the reactants. The site of the reaction is at the AO whose coefficient is largest in these frontier MO's. As seen from Table III, the HOMO of the $H_2(CH_3)Nb{=}CH_2$ has a maximum coefficient 0.57 at the p_π AO of the carbene carbon atom. On the other hand, the LUMO has a maximum coefficient 0.59 at the $5p_\pi$ AO of the Nb atom. Thus, the idea of frontier control enables us to predict easily the sites of the electrophilic and nucleophilic attacks to $H_2(CH_3)Nb{=}CH_2$. We note, however, a second possibility that the electrophile may also attack the Nb atom. The MO coefficient of the $4p_\pi$ MO is 0.49 in comparison with 0.57 for the p_π AO of the carbene carbon atom. In Figure 5, the contour map of the HOMO and the LUMO of $H_2(CH_3)Nb{=}CH_2$ are shown. The large amplitudes on C_{carb} in the HOMO and on Nb in the LUMO are illustrated.

Thus, from the present and previous studies,[12] we conclude that the reactivities of the metal carbene complexes are unifiedly explained by the frontier orbital theory, independent of whether the complex is either the Fischer type or the Schrock type.

Carbyne Complexes

Now, we show the results obtained for the carbyne complexes, $(CO)_5Cr{\equiv}CH^+$ and $Cl(CO)_4Cr{\equiv}CH$, which have the different reactivities as mentioned before. We report the properties of the $Cr{\equiv}C$ triple bond, the correlation diagram, charge distribution, and reactivity.

A. Properties of the Cr≡C Bond. For $(CO)_5Cr{\equiv}CH^+$, we have examined the two geometries because Huttner et al. reported

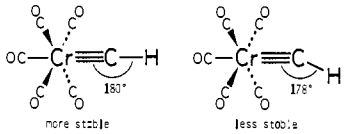

a non-linear M≡C–R bond from X-ray experiments on the complex *trans*-$[PMe_3(CO)_4CrCMe]BCl_4$.[23] The present calculation shows that the linear geometry is more stable than the bent one. Thus, the bent geometry would not be due to the bonding nature of the metal carbyne bond itself, but due to the other factors, for example, intermolecular interactions in the crystal.

In Table VII we summarize the properties of the Cr≡C triple bond. These results all imply the considerable strength of the Cr≡C triple bond in comparison with the Cr=C double bond or the Nb=C double bond. The bond length of the Cr≡C triple bond is calculated at 1.62–1.65 Å which agrees well with the experimental value, 1.69 Å, observed for $I(CO)_4Cr{\equiv}CCH_3$.[33]

Table VII. Properties of the Cr≡C Bonds in $(CO)_5Cr{\equiv}CH^+$ and $Cl(CO)_4Cr{\equiv}CH$

properties	$(CO)_5Cr{\equiv}CH^+$	$Cl(CO)_4Cr{\equiv}CH$
bond-dissocation energy, kcal/mol	175[a]	
bond length, Å	1.65	1.62[b]
force constant		
k, mdyn/Å	7.08	8.57
ω,[c] cm^{-1}	990–1110	1070–1190

[a] Dissociation energy to the singlet closed-shell fragments. [b] The experimental value is 1.69 Å for $I(CO)_4Cr{\equiv}CCH_3$. [c] The vibrational frequency was calculated from the force constant in two approximations; the atoms and groups of atoms bonded to the metal and the carbyne carbon atom are considered to completely follow or not to follow the vibration. The former approximation gives a minimum value and the latter a maximum one.

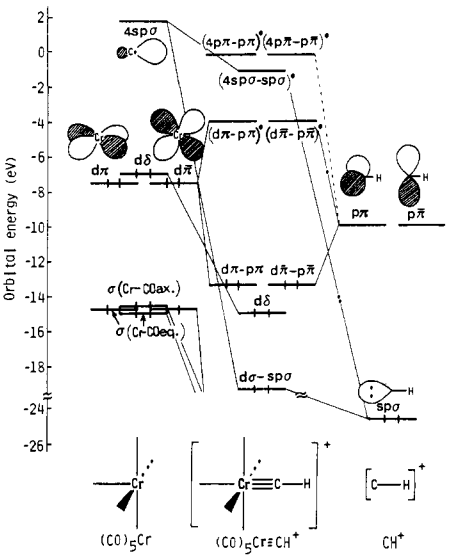

Figure 6. Correlation diagram of the orbitals of $(CO)_5Cr{\equiv}CH^+$ with those of the singlet fragments.

This length is shorter by 0.35 Å than the Cr=C double bond length 2.04 Å,[34] which is again shorter by 0.17 Å than the Cr–C single bond length, 2.21 Å.[35] The calculated force constant (7.1–8.6 mdyn/Å) is again much larger than that of the Cr=C double bond (1.6 mdyn/Å).[12] In addition, we also see the difference of the trans influences of Cl and CO ligands. The Cr≡C bond length is a little longer in $(CO)_5Cr{\equiv}CH^+$ than in $Cl(CO)_4Cr{\equiv}CH$ and the vibrational frequency is smaller in $(CO)_5Cr{\equiv}CH^+$ than in $Cl(CO)_4Cr{\equiv}CH$. These trends are in accord with those expected from the so-called trans effect.[36]

We calculated the Cr≡C bond energy of $(CO)_5Cr{\equiv}CH^+$ from its closed-shell singlet fragments, $(CO)_5Cr$ and CH^+, to be 175 kcal/mol. For $Cl(CO)_4Cr{\equiv}CH$, the Cr≡C bond energies corresponding to the fissions into the doublet and quartet fragments are 57.7 and 41.1 kcal/mol, respectively. These values based on the multiplet fragments should be underestimates, because we did not consider the electron-correlation effects. The calculation of the correlated wave function is necessary for more detailed discussion of the bond energy.

B. Correlation Diagram. We show in Figure 6 a correlation diagram of the orbitals of $(CO)_5Cr{\equiv}CH^+$ with those of its singlet fragments. Table VIII shows the orbital energies and the coefficients of some important MO's of the complex and its fragments. The HOMO of the CH^+ fragment is the sp_σ-hybrid lone pair on the carbon and the LUMO is the degenerate p_π and $p\pi$ (p_x, p_y)

(32) Fukui, K.; Yonezawa, T.; Shingu, H. *J. Chem. Phys.* **1952**, *20*, 722. Fukui, K. "Theory of Orientation and Stereoselection"; Splinger-Verlag: Berlin, 1975.

(33) (a) Fischer, E. O.; Kreis, G.; Kreiter, C. G.; Muller, J.; Huttner, G.; Lorentz, H. *Angew. Chem.* **1973**, *85*, 618; *Angew. Chem., Int. Ed. Engl.* **1973**, *12*, 564. (b) Huttner, G.; Lorentz, H.; Gartzke, W. *Angew. Chem.* **1974**, *86*, 667; *Angew. Chem., Int. Ed. Engl.* **1974**, *13*, 609.

(34) Mills, O. S.; Redhouse, A. D. *J. Chem. Soc. A* **1968**, 642.

(35) Cotton, F. A.; Richardson, D. C. *Inorg. Chem.* **1966**, *5*, 1851–1854.

(36) See p 1200 in ref 1.

Table VIII. Orbital Energies and Coefficients of Some Important MO's of $(CO)_5Cr{\equiv}CH^+$ and Its Singlet Fragments, $(CO)_5Cr$ and CH^+

	$(CO)_5Cr{\equiv}CH^+$			$(CO)_5Cr$			CH^+	
	Cr≡C (σ)	HOMO (π)	LUMO (π)	next HOMO (π)	HOMO (δ)	LUMO (nσ)	HOMO (nσ)	LUMO (π)
ϵ_i, eV	−18.913	−14.770	−2.373	−7.534	−6.909	1.731	−24.579	−9.880
Cr								
$3d_{x^2}$	−0.11	0.0	0.0	0.0	0.65	−0.15		
$3d_{y^2}$	−0.11	0.0	0.0	0.0	−0.65	−0.15		
$3d_{z^2}$	0.22	0.0	0.0	0.0	0.0	0.15		
$3d_{xy}$	0.0	0.0	0.0	0.0	0.0	0.0		
$3d_{xz}$	0.0	0.66	0.33	0.85	0.0	0.0		
$3d_{yz}$	0.0	0.0	0.0	0.0	0.0	0.0		
4s	−0.02	0.0	0.0	0.0	0.0	0.41		
$4p_x$	0.0	−0.03	0.46	−0.01	0.0	0.0		
$4p_y$	0.0	0.0	0.0	0.0	0.0	0.0		
$4p_z$	−0.04	0.0	0.0	0.0	0.0	0.77		
C(carbyne)								
2s	−0.40	0.0	0.0				0.60	0.0
$2p_x$	0.0	−0.49	0.63				0.0	1.0
$2p_y$	0.0	0.0	0.0				0.0	0.0
$2p_z$	−0.63	0.0	0.0				0.73	0.0
C(axial)								
2s	−0.34	0.0	0.0	0.0	0.0	0.27		
$2p_x$	0.0	0.06	0.40	0.14	0.0	0.0		
$2p_y$	0.0	0.0	0.0	0.0	0.0	0.0		
$2p_z$	−0.27	0.0	0.0	0.0	0.0	0.01		
C(equatorial)								
2s	−0.02	0.08	−0.28	0.0	0.0	−0.12		
$2p_x$	0.01	0.03	0.12	0.01	0.24	0.07		
$2p_y$	−0.01	−0.03	−0.07	−0.01	−0.24	−0.07		
$2p_z$	−0.04	0.05	0.07	0.10	0.0	0.14		

[a] See Figure 1 for the coordinates.

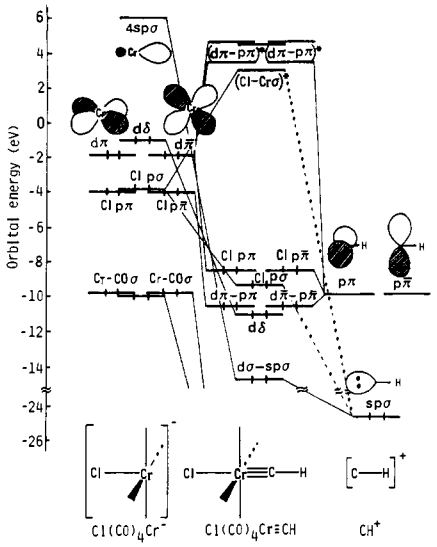

Figure 7. Correlation diagram of the orbitals of $Cl(CO)_4Cr{\equiv}CH$ with those of the singlet fragments.

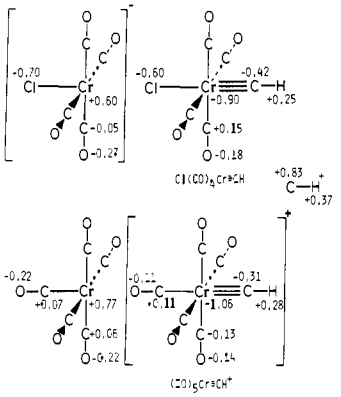

Figure 8. Net gross atomic charges in $Cl(CO)_4Cr{\equiv}CH$, $(CO)_5Cr{\equiv}CH^+$, and their singlet fragments.

orbitals on the carbon. The HOMO of the $(CO)_5Cr$ fragment is the d_δ-type lone-pair orbital and the next HOMO is the degenerate d_π- and $d\pi$ (d_{xz}, d_{yz})-type lone-pair orbitals. The LUMO is the $5sp_\sigma$-hybrid orbital of Cr extending outward. The MO's of $(CO)_5Cr{\equiv}CH^+$ are correlated with the MO's of the singlet fragments as follows. By a σ transfer of an electron from the HOMO of the CH^+ fragment to the LUMO of the $(CO)_5Cr$ fragment, the Cr≡C σ bond is formed and it is a d_σ–sp_σ bond. The degenerate two π bonds between Cr and C(carbyne) are formed through π back transfer from the degenerate next HOMO's of $(CO)_5Cr$ to the LUMO's of CH^+ and the bonds are d_π–p_π bonds. These transfers of electrons are an origin of the Cr≡C triple bond in $(CO)_5Cr{\equiv}CH^+$. The correlation diagram for $(CO)_5Cr{\equiv}CH^+$ is essentially the same as that for the Fischer-type carbene complex, $(CO)_5Cr{=}CH(OH)$.

Figure 7 shows the orbital correlation diagram for $Cl(CO)_4Cr{\equiv}CH$ with its closed-shell singlet fragments. Though the nature of the correlation is qualitatively similar to the case of $(CO)_5Cr{\equiv}CH^+$, the MO's in the frontier region are different between $Cl(CO)_4Cr{\equiv}CH$ and $(CO)_5Cr{\equiv}CH^+$. Table IX shows the energies and the coefficients of some important MO's of $Cl(CO)_4Cr{\equiv}CH$. The HOMO's of $(CO)_5Cr{\equiv}CH^+$ are the degenerate Cr≡C π-bonding MO's and the LUMO is the Cr≡C π-antibonding MO's, while the HOMO's of $Cl(CO)_4Cr{\equiv}CH$ are the degenerate Cl p_π- and $p\pi$-type lone-pair orbitals and the LUMO is the Cr–Cl σ-antibonding MO. The Cr≡C π-bonding MO's of $Cl(CO)_4Cr{\equiv}CH$ are lower in orbital energy than the Cl p_π- and $p\pi$-type lone pairs and the Cr≡C σ-antibonding MO is higher than the Cr–Cl σ-antibonding MO. This pattern of MO's reflects the fact that the Cr≡C bond is stronger than the Cr–Cl bond. If the interaction between Cr and Cl^- were stronger, the Cr–Cl π-bonding MO's would be more stable and the Cr–Cl σ-antibonding MO would be more unstable. Therefore, this difference between $Cl(CO)_4Cr{\equiv}CH$ and $(CO)_5Cr{\equiv}CH^+$ is also the result reflecting the difference of the trans effect of Cl^- and CO. These differences in the nature of the frontier MO's between $Cl(CO)_4Cr{\equiv}CH$ and $(CO)_5Cr{\equiv}CH^+$ will explain the difference of the reactivities of these two complexes, as will be shown below.

C. Charge Distribution. Figure 8 shows the atomic charges of $(CO)_5Cr{\equiv}CH^+$ and $Cl(CO)_4Cr{\equiv}CH$. With regard to the

Table IX. Orbital Energies and Coefficients of Some Important MO's of $Cl(CO)_4Cr{\equiv}CH$ and Its Singlet Fragments, $Cl(CO)_4Cr^-$ and CH^+

	$Cl(CO)_4Cr{\equiv}CH$					$Cl(CO)_4Cr^-$			CH^+	
	Cr≡C (σ)	Cr≡C (π)	HOMO	LUMO	next LUMO (π)	next HOMO (π)	HOMO (δ)	LUMO ($n\sigma$)	HOMO ($n\sigma$)	LUMO (π)
ϵ_i eV	−14.825	−10.552	−8.504	2.990	3.488	−1.979	−1.037	6.061	−24.579	−9.880
Cr										
$3d_{x^2}$	−0.20	0.0	0.0	0.0	0.0	0.0	0.57	−0.18		
$3d_{y^2}$	−0.20	0.0	0.0	0.0	0.0	0.0	−0.57	−0.18		
$3d_{z^2}$	0.41	0.0	0.0	0.26	0.0	0.0	0.0	0.04		
$3d_{xy}$	0.0	0.0	0.0	0.0	0.0	0.0	0.0	0.0		
$3d_{xz}$	0.0	0.58	0.28	0.0	0.45	0.80	0.0	0.0		
$3d_{yz}$	0.0	0.0	0.0	0.0	0.0	0.0	0.0	0.0		
4s	0.0	0.0	0.0	−0.22	0.0	0.0	0.0	0.63		
$4p_x$	0.0	0.0	−0.13	0.0	−0.05	0.11	0.0	0.0		
$4p_y$	0.0	0.0	0.0	0.0	0.0	0.0	0.0	0.0		
$4p_z$	0.0	0.0	0.0	0.65	0.0	0.0	0.0	−0.76		
C(carbyne)										
2s	0.39	0.0	0.0	0.39	0.0				0.60	0.0
$2p_x$	0.0	0.47	−0.28	0.0	−0.47				0.0	−1.0
$2p_y$	0.0	0.0	0.0	0.0	0.0				0.0	0.0
$2p_z$	0.65	0.0	0.0	0.03	0.0				0.73	0.0
Cl										
3s	−0.08	0.0	0.0	−0.33	0.0	0.0	0.0	0.22		
$3p_x$	0.0	0.43	−0.90	0.0	0.22	−0.54	0.0	0.0		
$3p_y$	0.0	0.0	0.0	0.0	0.0	0.0	0.0	0.0		
$3p_z$	−0.11	0.0	0.0	0.35	0.0	0.0	0.0	−0.12		
C(equatorial)										
2s	−0.07	0.05	0.14	0.08	0.27	−0.03	0.0	−0.18		
$2p_x$	0.04	−0.02	−0.05	0.03	−0.25	−0.04	−0.16	−0.05		
$2p_y$	−0.04	0.02	0.05	0.0	−0.04	0.0	0.16	0.05		
$2p_z$	0.02	0.05	0.02	0.29	−0.07	−0.11	0.0	−0.12		

[a] See Figure 1 for the coordinates.

Table X. σ and π AO Populations of the Carbyne, CO, and Cl Ligands in Free States, $(CO)_5Cr{\equiv}CH^+$, and $Cl(CO)_4Cr{\equiv}CH$[a]

ligand	free	$(CO)_5Cr{\equiv}CH^+$	$Cl(CO)_4Cr{\equiv}CH$
CH^+			
σ	6.0	5.672 (−0.328)	5.573 (−0.427)
π	0.0	1.353 (+1.353)	1.594 (+1.594)
CO (axial)			
σ	10.0	9.851 (−0.149)	
π	4.0	4.149 (+0.149)	
CO (equatorial)			
σ	10.0	9.815 (−0.185)	9.836 (−0.164)
π	4.0	4.193 (+0.193)	4.197 (+0.197)
Cl^-			
σ	10.0		9.727 (−0.273)
π	8.0		7.875 (−0.125)

[a] Values in parentheses show the amounts of the transfer (negative) and back transfer (positive) from the ligand to the Cr atom.

charge distribution of the cationic carbyne complexes, the idea that the carbyne carbon atom has a large positive charge has been commonly accepted.[4] This estimation is based on the fact that the nucleophilic attack is exclusively observed at the carbyne carbon atom. However, our calculated results shown in Figure 8 show that the atomic charge of the carbyne carbon is significantly negative, 0.42− for $Cl(CO)_4Cr{\equiv}CH$ and 0.31− even for the cationic carbyne complex $(CO)_5Cr{\equiv}CH^+$, contrary to the commonly accepted idea. Even considering the ambiguity of population analysis, it would safely be said that the carbyne carbon atom is more negative than the other carbonyl carbons. The Cr atom is positively charged, for example, by 0.77 in the $(CO)_5Cr$ fragment and by 1.06 in the $(CO)_5Cr{\equiv}CH^+$.

Table X shows an analysis of σ and π charges of the ligands. It shows that the large negative charges on the carbyne carbon atoms in the complexes are due to the large π back transfer from the $(CO)_5Cr$ fragment or the $Cl(CO)_4Cr$ fragment to the CH^+ fragment, the σ transfers are not so large. For the CO ligands, the amounts of σ transfer and π back transfer of electrons are almost balanced for both in axial and equatorial positions. For the equatorial CO, the interaction seems to be larger than that for the axial CO. Table XI shows the AO populations of the metal atom. It is seen that in both complexes a decrease of the population in d_π and $d\pi$ (d_{xz}, d_{xy}) AO's and an increase of the population in d_σ (d_{z^2}) AO occur, as expected, by the Cr≡C bond formation.

Table XI. Valence AO Populations of the Cr Atoms of $(CO)_5Cr{\equiv}CH^+$, $Cl(CO)_4Cr{\equiv}CH$, and Their Fragments[a,b]

	$(CO)_5Cr{\equiv}CH^+$		$Cl(CO)_4Cr{\equiv}CH$	
AO	fragment	complex	fragment	complex
$3d_{x^2}$	0.18	0.25	0.17	0.26
$3d_{y^2}$	0.18	0.25	0.17	0.26
$3d_{z^2}$	0.08	0.40	0.04	0.46
$3d_{xy}$	1.31	1.72	1.04	1.72
$3d_{xz}$	1.58	1.09	1.74	1.03
$3d_{yz}$	1.58	1.09	1.74	1.03
sum	4.91	4.80	4.90	4.76
4s	0.07	−0.02	0.12	0.02
$4p_x$	0.08	0.04	0.13	0.09
$4p_y$	0.08	0.04	0.13	0.09
$4p_z$	0.04	0.0	0.08	0.07
sum	0.27	0.06	0.46	0.27

[a] See Figure 1 for the coordinates. [b] The electron configuration of the Cr atom is d^5s^1.

Table XII. Analysis of the Charge of the Carbyne Carbon Atom

molecule[a]	population π	population σ	population $\pi + \sigma$	atomic charge
$(CO)_5Cr{\equiv}C^*H^+$	1.353	4.954	6.307	−0.307
$Cl(CO)_4Cr{\equiv}C^*H$	1.594	4.825	6.419	−0.419
$HC{\equiv}C^*H$	2.0	4.317	6.317	−0.317

[a] The charge on the carbon with an asterisk is analyzed.

Table XII shows an analysis of the charges of the carbyne carbon atoms into σ and π components. As a standard population of the carbyne carbon atom, we showed the σ and π populations of the carbon atom in acetylene. The component which mainly contributes to the negative charges of the carbyne carbon atoms is the π component. As compared with the π component population of the carbyne carbon in $HC{\equiv}CH$, the π component in $(CO)_5Cr{\equiv}CH^+$ or $Cl(CO)_4Cr{\equiv}CH$ is rather small. Thus, though the carbyne carbon atoms in these complexes have negative

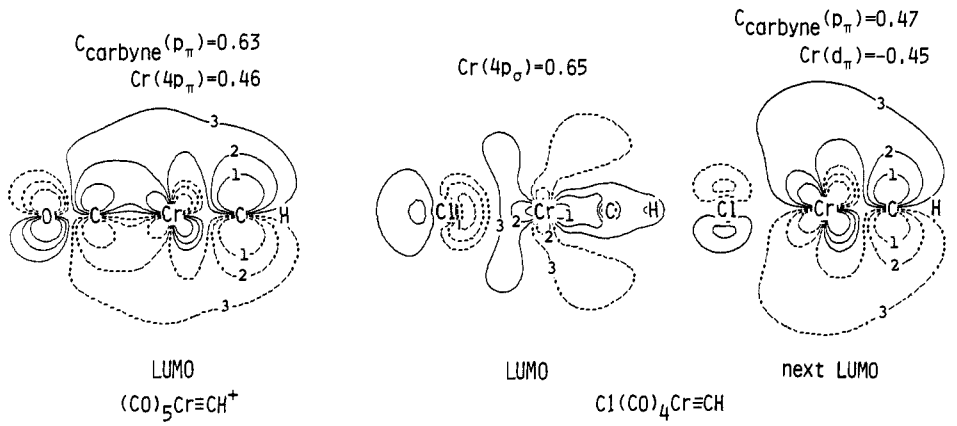

Figure 9. Contour maps of the frontier orbitals of $(CO)_5Cr{\equiv}CH^+$ and $Cl(CO)_4Cr{\equiv}CH$. The intersection includes the Cr≡C bond and lies at an angle of 45° with x or y axes. Solid and broken lines correspond to plus and minus signs in the MO's. The numbers 1–3 on the contours correspond to the values (au) 0.1, 0.05, and 0.02, respectively. Above each map, the dominant coefficients of the orbital are shown.

atomic charges, they are electron deficient in the π region. When a nucleophile attacks the carbyne carbon atom from the π direction, it can see the nuclear positive charge. From this analysis, an attack of the nucleophile at the carbyne carbon atom may be understood as "regional" charge-controlled reactions. However, we will see in the next section that this analysis is only another expression of the idea of frontier orbital (LUMO) control. We have shown in a previous paper a similar situation in the charge distribution and reactivity of the Fischer-type carbene complexes.[12]

D. Reactivity. It is reported that the reactivities of the cationic and neutral carbyne complexes are different.[4] The cationic carbyne complexes are amenable to attack of nucleophiles exclusively at the carbyne carbon atom. For example, $(CO)_5Cr{\equiv}C{-}N(C_2H_5)_2^+$ reacts as follows.[37] On the other hand, the neutral

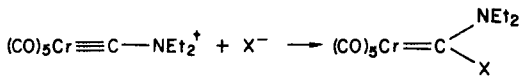

carbyne complexes show very different reactivities to nucleophiles. Depending on the nucleophilicity of the reactant, the attack at the carbyne carbon atom[38] or the substitution of the CO ligand[39] or the *trans*-positioned halide ligand[4] occurs.

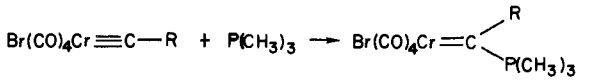

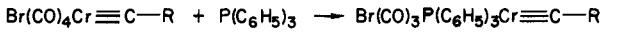

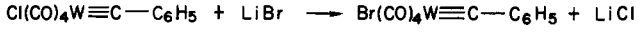

Here, the nucleophilicity of $P(CH_3)_3$ is stronger than that of $P(C_6H_5)_3$.

From these experiments, the reactivity of the cationic carbyne complexes was thought to be due to the positive charge localized at the carbyne carbon atom. The origin of the different reactivities of the neutral carbyne complexes was not obvious. However, the atomic charge of the carbyne carbon atom calculated here is significantly negative not only for the neutral carbyne complex but also for the cationic carbyne complex (Figure 8). The present results show that the idea of charge control of the reaction is erroneous. On the basis of the frontier orbital theory, the primary feature of the reaction of the nucleophile and the metal carbyne complex should be determined by the LUMO of the complex. The nucleophile attacks the atom at which the coefficient of the LUMO is maximum. As seen from Tables VIII and IX, the maximum coefficient in the LUMO is at the carbyne carbon atom in the cationic carbyne complex, $(CO)_5Cr{\equiv}CH^+$, but at the Cr atom in the neutral one, $Cl(CO)_4Cr{\equiv}CH$. In addition, for $Cl(CO)_4Cr{\equiv}CH$, the LUMO and the next LUMO are energetically very close. The difference of the orbital energy is only 0.498 eV, but the corresponding difference for $(CO)_5Cr{\equiv}CH^+$ is 1.353 eV. In the next LUMO of $Cl(CO)_4Cr{\equiv}CH$, the $2p_\pi$ AO on the carbyne carbon has the maximum coefficient. Thus, the reactivities of the carbyne complexes are understood as follows. The reactivity of the cationic carbyne complex is frontier controlled. This is very similar to the case of the Fischer-type carbene complex. For the neutral carbyne complex, its reactivity is also understood on the basis of the frontier orbital theory. When the nucleophilic reagent is strong, it would be able to attack both the Cr and carbyne carbon atoms because of the very small energy separation between the LUMO and the next LUMO. On the other hand, a weak nucleophile would attack only the Cr atom where the LUMO has the maximum coefficient. Thus, the difference of the reactivity between the cationic and neutral complexes is understood from the difference in the nature of the frontier MO's between the two kinds of complexes.

Figure 9 shows the contour maps of the frontier MO's: the LUMO of $(CO)_5Cr{\equiv}CH^+$ and the LUMO and the next LUMO of $Cl(CO)_4Cr{\equiv}CH$. The contour map of the LUMO of $(CO)_5Cr{\equiv}CH^+$ is very similar to that of the Fischer-type carbene complex, $(CO)_5Cr{=}CH(OH)$, and it shows a large amplitude at the carbyne carbon atom. On the other hand, the LUMO of $Cl(CO)_4Cr{\equiv}CH$ is localized on the d orbital of the Cr atom, but the next LUMO is localized on both the carbyne carbon and chromium atom. Thus, the reactivity of the carbyne complexes is understood as frontier controlled.

Conclusion

In the present work, we have investigated the natures and reactivities of the metal–carbon multiple bonds in the Schrock-type carbene complex $H_2(CH_3)Nb{=}CH_2$ and the carbyne complexes $(CO)_5Cr{\equiv}CH^+$ and $Cl(CO)_4Cr{\equiv}CH$.

The $M{=}C_{carb}$ bond in the Schrock-type carbene complex is stronger than that in the Fischer-type carbene complex. The properties calculated for the $Nb{=}C_{carb}$ bond, i.e., the rotational barrier, bond length, bond-dissociation energy, and force constant, compare reasonably well with the available experimental data obtained for the related complexes. The nature of the $Nb{=}C_{carb}$ bond is studied by the orbital-correlation diagram. The origin of the large rotational barrier of the $Nb{=}C_{carb}$ bond is understood from the absence of the degenerate d_π- and $d\pi$-type lone-pair MO's for the $H_2(CH_3)Nb$ fragment. The polarization of the charge in the $Nb{=}C_{carb}$ bond is calculated to be Nb(0.10–)=C(0.66–). The reactivity of the Schrock-type carbene complex is shown to be frontier controlled as for the Fischer-type carbene complexes. The HOMO has a maximum coefficient on the C_{carb} atom, and the LUMO has a maximum coefficient on the Nb atom. Therefore, an electrophile attacks the C_{carb} atom and a nucleophile attacks the Nb atom.

(37) Fischer, E. O.; Kleine, W.; Kreissl, F. R. *Angew. Chem.* **1976**, *88*, 646–647.
(38) Kreissl, F. R. *J. Organomet. Chem.* **1975**, *99*, 305–308.
(39) Fischer, E. O.; Ruhs, A.; Kreissl, F. R. *Chem. Ber.* **1977**, *110*, 805–815.

Next, we studied the Cr≡C triple bond in the cationic and neutral metal carbyne complexes, $(CO)_5Cr{\equiv}CH^+$ and $Cl(CO)_4Cr{\equiv}CH$, respectively, which show different reactivities for nucleophiles. The nature of the Cr≡C bond studied by the orbital-correlation diagram is similar to that of the M=C bond in the Fischer-type carbene complexes. The polarization of the Cr≡C bond is calculated to be Cr(1.06+)—C(0.31−) for $(CO)_5Cr{\equiv}CH^+$ and Cr(0.90+)—C(0.42−) for $Cl(CO)_4Cr{\equiv}CH$. Just as the Fischer-type carbene complex, the carbyne carbon atom is negatively charged in contradiction with the idea of the charge-controlled reactivity. The reactivity of the carbyne complexes can be explained clearly by the frontier orbital theory. The differences in the reactivity between the cationic and neutral carbyne complexes are explained from the existence of the nearly degenerate LUMO and next LUMO in the frontier MO region of the neutral complex. They would never be explained by the charge-controlled mechanism.

Thus, the nature of the metal–carbon multiple bonds in the Fischer-type and Schrock-type carbene complexes and in the carbyne complex has been clarified theoretically by the previous[12] and present studies. The reactivities of these metal–carbon multiple bonds are understood in a unified form on the basis of the frontier orbital theory.

Acknowledgment. For the SCF calculations we have used a slightly modified version of the HONDOG program by King, Dupuis, and Rys whom the author would like to acknowledge. Calculations were carried out with the HITAC M-200H computer at the Institute for Molecular Science and with the FACOM M-382 computer at the Data Processing Center of Kyoto University. Part of this study was supported by the Japan Society for the Promotion of Science.

Registry No. $H_2(CH_3)Nb{=}CH_2$, 91711-58-9; $(CO)_5Cr{\equiv}CH^+$, 91711-56-7; $Cl(CO)_4Cr{\equiv}CH$, 91711-57-8.

Theoretical Study of Multiple Metal–Metal Bonds in Binuclear Complexes of Group 6D and Group 7D Transition Elements with the General Formula $M_2Cl_4(PH_3)_4^{n+}$ (n = 0, 1, 2) by the Hartree–Fock–Slater Transition-State Method

Tom Ziegler

Contribution from the Department of Chemistry, University of Calgary, 2500 University Drive N.W., Calgary, Alberta, Canada T2N 1N4. *Received January 18, 1984*

Abstract: Hartree–Fock–Slater calculations are reported on $M_2Cl_4(PH_3)_4^{n+}$ for M = Mn, Tc, Re with n = 0, 1, 2, as well as for M = Mo with n = 0, 1 and M = Cr, W with n = 0. The calculated metal–metal bond energies for n = 0 are $D(Cr{\overset{4}{-}}Cr)$ = 153 kJ mol^{-1}, $D(Mo{\overset{4}{-}}Mo)$ = 524 kJ mol^{-1}, and $D(W{\overset{4}{-}}W)$ = 428 kJ mol^{-1}, respectively. The calculated bond strengths in $M_2Cl_4(PH_3)_4$ for M = Mn, Tc, and Re were $D(Mn{\overset{4}{-}}Mn)$ = 295 kJ mol^{-1}, $D(Tc{\overset{4}{-}}Tc)$ = 599 kJ mol^{-1}, and $D(Re{\overset{4}{-}}Re)$ = 562 kJ mol^{-1}, respectively. An energy-decomposition analysis provided a possible explanation for the relative strength of the metal–metal bond between 3d, 4d, and 5d elements. The analysis indicated further that the δ bond is rather weak. The contribution from relativistic effects to the metal–metal bond in the binuclear complexes of 5d elements was calculated to be small.

I. Introduction

The number of well-characterized binuclear complexes[1] of the general formula $M_2(X)_m(L)_{8-m}^{n+}$, where X represents halides and L phosphines, has grown considerably over the past 20 years, following the recognition[2] of a quadrupole bond in $Re_2Cl_8^{2-}$. It is now known[1] that W, Mo, Re, and to some extent Tc can form binuclear complexes of the type $M_2(X)_m(L)_{8-m}^{n+}$ in which the metal–metal bond order is 3, 3.5, and 4, whereas $M_2(X)_m(L)_{8-m}^{n+}$ systems of either Cr or Mn are unknown.

Cotton[2] described in 1965 the quadrupole bond of $Re_2Cl_8^{2-}$ in terms of one σ bond, two π bonds, and one δ bond. The essence of this bonding scheme has since been confirmed by SCF-Xα-SW calculations[3] on several $M_2(X)_m(L)_{8-m}^{n+}$ systems. However, a number of recent theoretical works[4] have shown that a simple molecular orbital picture is inadequate for a quantitative description of the weak δ bond.

Theoretical investigations to date have concentrated mainly on the assignment of electronic spectra. There has been much less emphasis on an evaluation of the metal–metal bond strength.[5] This is in a way unfortunate since it has proven difficult experimentally[1a] to assess metal–metal bond energies. There is as a consequence not a clear understanding of how the σ component, the two π components, and the δ component contribute in relative terms to the bond strength. Lack of experimental and theoretical data has also made it difficult to evaluate[1b] variations in the bond strength between 3d, 4d, and 5d elements.

The Xα method as implemented by Baerends[6] et al. (LCAO-HFS method) has previously, in connection with the generalized

(1) (a) Cotton, F. A.; Walton, R. A. "Multiple Bonds Between Metal Atoms"; Wiley: New York, 1982. (b) Cotton, F. A. *Chem. Soc. Rev.* **1983**, *12*, 35.

(2) Cotton, F. A. *Inorg. Chem.* **1965**, *4*, 334.

(3) (a) Norman, J. G., Jr.; Kolari, H. J. *J. Am. Chem. Soc.* **1975**, *97*, 33. (b) Mortala, A. P.; Moskowitz, J. W.; Rosch, N.; Cowan, C. D.; Gray, H. B. *Chem. Phys. Lett.* **1975**, *32*, 283. (c) Cotton, F. A.; Hubbard, J. L.; Lichtenberger, D. L.; Shim, I. *J. Am. Chem. Soc.* **1982**, *104*, 679. (d) Bursten, B. E.; Cotton, F. A.; Fanwick, P. E.; Stanley, G. G. *J. Am. Chem. Soc.* **1983**, *105*, 3082. (e) Bursten, B. E.; Cotton, F. A.; Fanwick, P. E.; Stanley, G. G.; Walton, R. A. *J. Am. Chem. Soc.* **1983**, *105*, 2606.

(4) (a) Benard, M.; Veillard, A. *Nouv. J. Chim.* **1977**, *1*, 97. (b) Guest, M. F.; Hillier, I. H.; Garner, C. D. *Chem. Phys. Lett.* **1977**, *48*, 587. (c) Hay, P. J. *J. Am. Chem. Soc.* **1978**, *100*, 2897. (d) Correa de Mello, P.; Edwards, W. D.; Zerner, M. C. *J. Am. Chem. Soc.* **1982**, *104*, 1440. (e) Hay, P. J. *J. Am. Chem. Soc.* **1982**, *104*, 7007. (f) Hall, M. B. *J. Am. Chem. Soc.* **1980**, *102*, 2104.

(5) (a) Kok, R. A.; Hall, M. B. *Inorg. Chem.* **1983**, *22*, 728. (b) Ziegler, T. *J. Am. Chem. Soc.* **1983**, *105*, 7543. (c) Goodgame, M. M.; Goddard, W. A. *J. Phys. Chem.* **1981**, *85*, 215. (d) Delley, B.; Ellis, D. E. *Phys. Rev. Lett.* **1983**, *50*, 488.

(6) (a) Baerends, E. J.; Ellis, D. E.; Ros, P. *Chem. Phys.* **1973**, *2*, 41. (b) Baerends, E. J.; Ros, P. *Int. J. Quantum Chem.* **1978**, *S12*, 169.

0002-7863/84/1506-5901$01.50/0